land

Article

Assessment of Coastal Carbon Storage and Analysis of Its Driving Factors: A Case Study of Jiaozhou Bay, China

Longkun Zhang, Qingchun Guan *, Hui Li, Junwen Chen, Tianya Meng and Xu Zhou

College of Oceanography and Space Informatics, China University of Petroleum (East China), Qingdao 266580, China; 2116020228@s.upc.edu.cn (L.Z.); z22160025@s.upc.edu.cn (H.L.); z23160019@s.upc.edu.cn (J.C.); z23160001@s.upc.edu.cn (T.M.); z23160044@s.upc.edu.cn (X.Z.)
* Correspondence: qingchunguan@upc.edu.cn

Abstract: Global climate change and coastal urbanization have significantly impacted the health and carbon storage of coastal zone ecosystems. Investigating the spatial and temporal variations in coastal carbon storage is crucial for developing effective strategies for land management and ecological protection. Current methods for evaluating carbon storage are hindered by insufficient accuracy and data acquisition challenges, necessitating solutions to enhance both reliability and precision. This study aims to assess the variations in carbon storage and annual carbon sequestration in the Jiaozhou Bay coastal zone from 1990 to 2020 and to identify the driving factors by integrating the Integrated Valuation of Ecosystem Services and Trade-offs (InVEST) and Carnegie Ames Stanford Approach (CASA) models with remote sensing data and geographic detector methods. The findings suggest that Jiaozhou Bay has experienced a substantial decrease in carbon storage, declining by 17.4% from 1990 to 2020, and annual carbon sequestration, decreasing by 35.5% from 1990 to 2016, but has stabilized recently. Vegetation cover and water bodies play critical roles in regional carbon storage. Furthermore, the dynamics of carbon storage and land use patterns are significantly influenced by socioeconomic factors, including GDP and population density. A comparison of the InVEST and CASA models demonstrates consistency in their carbon storage and annual carbon sequestration assessments. Combining these models in future assessments can enhance the scientific rigor and accuracy of the research, providing more reliable evidence for ecosystem management and policy making.

Keywords: coastal zone; blue carbon; ecosystem services; land use change; InVEST model; CASA model

Citation: Zhang, L.; Guan, Q.; Li, H.; Chen, J.; Meng, T.; Zhou, X. Assessment of Coastal Carbon Storage and Analysis of Its Driving Factors: A Case Study of Jiaozhou Bay, China. *Land* **2024**, *13*, 1208. https://doi.org/10.3390/land13081208

Academic Editors: Luis Diaz-Balteiro, César Pérez-Cruzado and Manuel Marey-Pérez

Received: 28 June 2024
Revised: 1 August 2024
Accepted: 3 August 2024
Published: 5 August 2024

1. Introduction

Coastal zone ecosystems have significant potential for carbon sequestration and storage, commonly referred to as coastal blue carbon. Blue carbon refers to the organic carbon captured and stored by marine and coastal ecosystems [1]. It is a crucial component of the ocean's carbon sink and provides various ecosystem functions and services, including coastal protection and climate regulation [2–5]. For example, although coastal zones account for only 0.2% of the world's oceans, they contribute half of the carbon burial in marine sediments [6]. As a key part of the ocean carbon sink, coastal zone ecosystems play a vital role in the global carbon cycle. Due to their high primary productivity and carbon storage potential, coastal blue carbon is considered a natural climate solution [7,8] and plays a vital role in the carbon cycle and in addressing global warming [6,9].

However, coastal zones are among the most vulnerable and threatened ecosystems, highly susceptible to both climate and nonclimate factors [10]. Global climate change and intensified human activities, especially urbanization and industrialization in coastal zones, pose a serious threat to the carbon sequestration capacity and ecosystem health of coastal zones [11]. These activities significantly reduce their carbon sequestration function [12], greatly weakening the role of coastal blue carbon ecosystems in addressing climate issues.

Studies have shown that LUCC (land use and cover change) can change the structure and function of ecosystems, thereby affecting changes in carbon storage [13,14]. At the same time, LUCC can destroy soil and vegetation, resulting in a large amount of carbon exchange, which impacts the carbon storage capacity of the ecosystem [15–17]. Carbon storage is closely related to ecosystem productivity and climate regulation, making it one of the key indicators for measuring the value of ecosystem services. Therefore, studying the spatiotemporal characteristics of blue carbon in coastal zones is crucial for effectively monitoring regional carbon changes and updating carbon budgets [18–20].

Currently, the assessment of carbon storage in coastal zone ecosystems is mainly conducted through field surveys [21], remote sensing inversion [22], and model simulation [23–25]. Although field surveys are accurate, they are only applicable to small areas, and the field sampling process is time-consuming and labor-intensive, making it difficult to achieve comparative analysis of past and present conditions and real-time monitoring of changes [26,27]. In contrast, remote sensing inversion methods can cover large areas and provide continuous monitoring, but they rely on high-quality data and advanced algorithms [28]. Model simulation methods are increasingly valued for their ability to effectively estimate and predict carbon storage at various scales. For example, Christopher Potter et al. used the CASA model to assess forest productivity in Southeast Asia [29]; Jiaqian Sun et al. used the BIOME-BGC model to conduct sensitivity analysis and parameter calibration of net ecosystem productivity (NEP) in China's subtropical forests, providing important technical support for the carbon sink function of subtropical forest ecosystems [30]; Maarten C. Braakhekke et al. used the Lund–Potsdam–Jena Managed Land (LPJmL) model to study the carbon absorption potential of global forest plantations, assessing the carbon accumulation capacity of temperate, tropical, and boreal plantations under different climatic conditions by simulating specific plantation functional types [31]. In recent years, the InVEST model has also been widely used in the assessment of ecosystem services [32]. Notably, the carbon storage and sequestration module can effectively estimate and analyze blue carbon in coastal zones, providing valuable decision-making support information [33]. Additionally, the CASA model effectively combines remote sensing data and meteorological data to estimate net primary productivity (*NPP*) using the driving forces of photosynthetically active radiation and vegetation photosynthetic efficiency. By integrating with the vegetation carbon sequestration model, CASA can accurately estimate the carbon sequestration of vegetation [34].

Although scholars have used the above models to assess carbon storage from multiple perspectives and scales, no research has been conducted to assess coastal blue carbon from the perspectives of both InVEST and CASA models. The InVEST model offers a detailed assessment of carbon storage by evaluating multiple carbon pools within the ecosystem, while the CASA model uses photosynthetically active radiation and light energy utilization to accurately estimate *NPP* and carbon sequestration on a large scale. Therefore, the two models have their respective strengths in assessing carbon storage and carbon sequestration. The former excels in providing detailed information on carbon pools, while the latter is superior for dynamic monitoring on a large scale. By combining these models, this study offers a comprehensive analysis of the storage and dynamic changes of coastal blue carbon from multiple perspectives, enhancing the accuracy and depth of carbon storage assessments. This approach allows for a more thorough and dynamic understanding of coastal carbon storage and sequestration. By applying these models to the Jiaozhou Bay coastal zone, a region significant for biodiversity and ecological protection, this research not only advances the methodology for carbon assessment but also provides valuable insights for regional ecological management and policy making. The Jiaozhou Bay coastal zone in China plays a significant role in international ecological protection. It provides a resting place or wintering ground for tens of thousands of migratory birds annually, serving as an important node in the global migration of migratory birds and a key ecological safeguard for regional sustainable development [35]. It is not only a critical protected area for biodiversity but also a key zone for regional climate regulation and carbon sequestration [36]. With the intensification of global climate change and human activities, the Jiaozhou Bay coastal zone faces numerous challenges. Among these, LUCC significantly impacts the ecological function and carbon storage capacity of the coastal zone amid rapid urbanization. Therefore, it is particularly important to study the changes in carbon storage in the Jiaozhou Bay coastal zone in depth, providing a scientific basis for the formulation of ecological protection measures in Jiaozhou Bay.

Therefore, this study selected Landsat image data from 1990, 2000, 2010, and 2020, extracted land use data using a random forests algorithm, and utilized the InVEST and CASA models to evaluate the spatiotemporal patterns of carbon storage in the Jiaozhou Bay coastal zone. GeoDetector was employed to identify the driving factors, and Pearson correlation analysis was conducted to analyze the relationships between different factors affecting carbon storage. The goal of this study is to provide decision support for the protection and land use adjustment strategies of the Jiaozhou Bay coastal zone, as well as for the sustainable management of the coastal zone. Figure 1 shows the overall research process of this study.

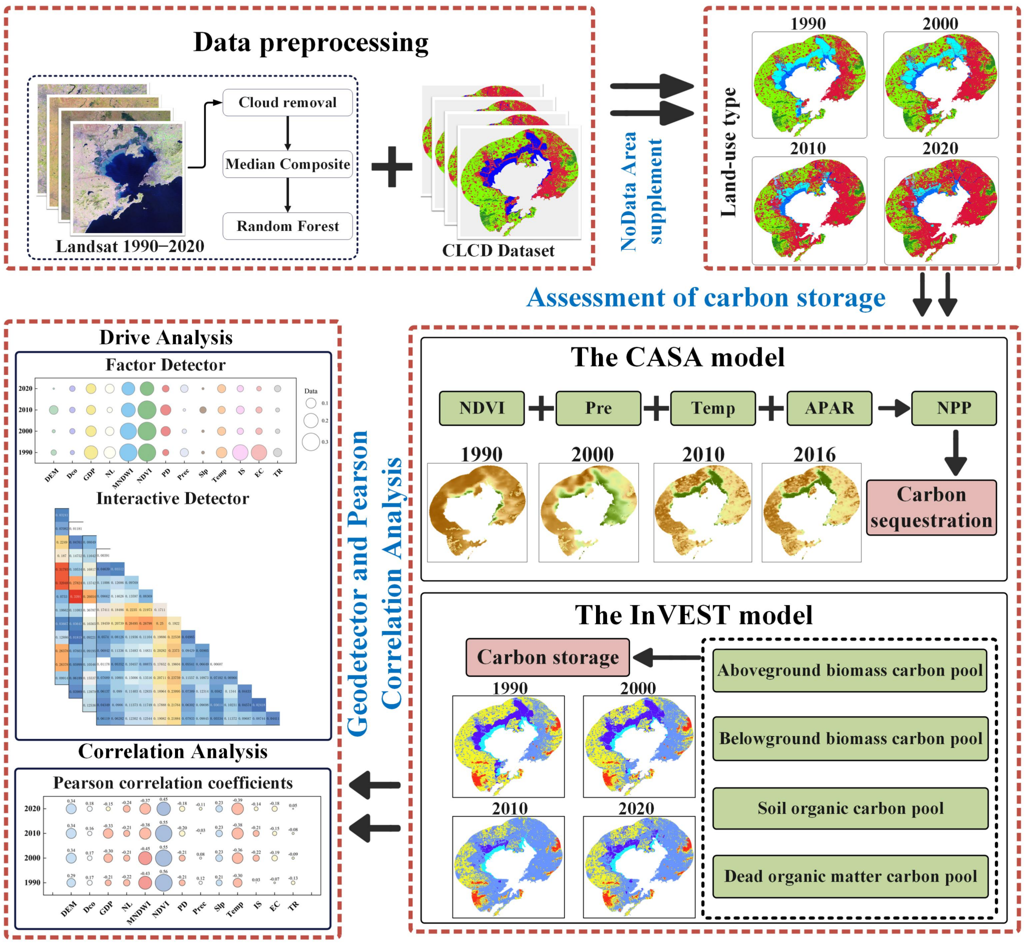

Figure 1. The framework of this study.

2. Materials and Methods

2.1. Study Area

Jiaozhou Bay, a semienclosed bay extending inland, is located on the southern coast of the Shandong Peninsula in China and connects to the Yellow Sea. The bay covers nearly 473 km^2, with an average depth of approximately 7 m and a maximum depth of 64 m. The region experiences a mild temperate monsoon climate with distinct oceanic characteristics, an average annual temperature of 12.2 °C, and an average annual rainfall of 776 mm [35]. The Jiaozhou Bay coastal wetlands are the largest estuarine bay-type wetlands in the

Jiaodong Peninsula, nourished by major rivers such as the Dagu, Baisha, Licun, Moshui, and Haipo Rivers. The wetlands in Jiaozhou Bay include salt marshes and seagrass beds. Important wetland plants include Spartina alterniflora in the salt marshes and Zostera marina in the seagrass beds. These plants play critical roles in sediment stabilization, coastal protection, and providing habitat for various wildlife species.

In recent years, land use and cover patterns in Jiaozhou Bay have been significantly altered due to accelerated urbanization. The continuous advancement of the land boundary into the bay has led to changes in tidal flat wetlands and a decline in the ecological quality of the coastal zone [36]. This investigation focuses on Jiaozhou Bay and its surrounding areas. Due to significant changes in the coastline in recent years [37], the land boundary of the study area was determined based on the 1990 coastline. Initially, the study area was determined based on the 1990 coastline and extended 10 km inland. For subsequent years, the study area comprises the land boundary of the 1990 area combined with the coastline of each respective year. While the overall study area remains largely consistent, slight variations occur due to changes in the coastline. The selection of this study area is based on the guidelines provided in the "Concise Rules for the Comprehensive Survey of Coastal Zone and Tideland Resources in China", ensuring the rationality and scientific basis of the chosen research area. The total area covered is approximately 1655 km^2 (119.99° E–120.49° E, 35.89° N–36.35° N) (Figure 2) [38].

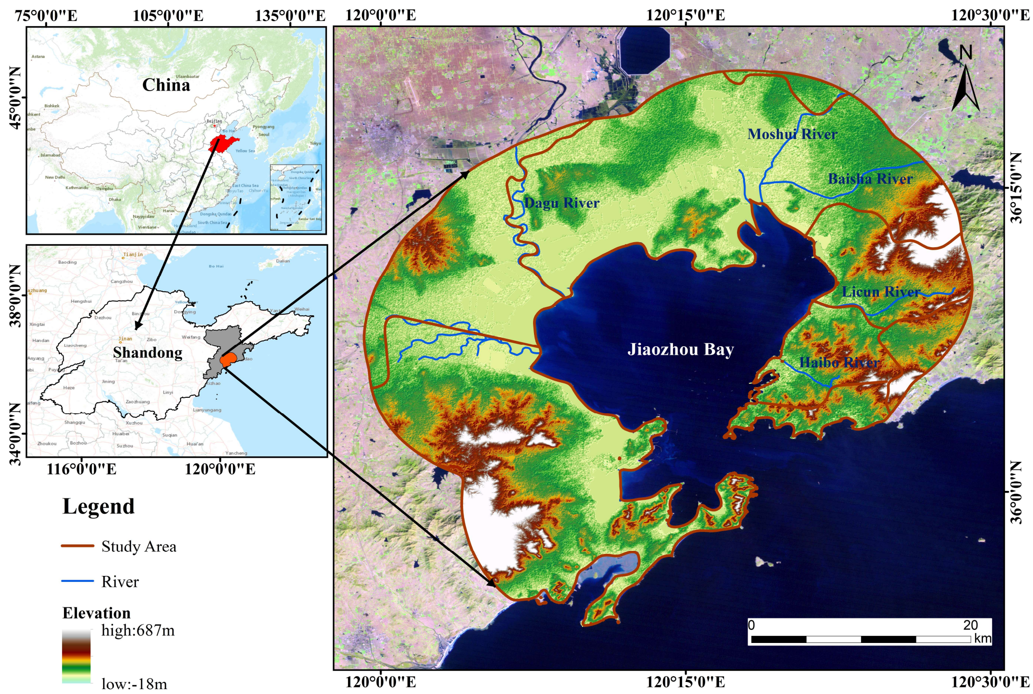

Figure 2. Jiaozhou Bay's terrain and location.

2.2. Data Sources

2.2.1. Source Information

This study includes the following data: (1) Remote sensing image data: Landsat series data from Google Earth Engine (GEE) were selected, including Landsat 5 and Landsat 8 images with a resolution of 30 m and cloud cover of less than 10% for the years 1990, 2000, 2010, and 2020. These images underwent declouding and median synthesis operations, and were subsequently integrated to create geometrically and atmospherically corrected remote sensing image datasets. (2) CLCD dataset: This supplementary dataset, derived from the AI Earth platform, includes nine categories: cropland, woodland, shrubs, grassland, water bodies, snow, bare ground, impervious surfaces, and wetlands. Its overall accuracy exceeds 80% and it spans the years 1985 and 1990–2021, making it well suited for this analysis [39].

(3) Meteorological data: Various meteorological data, including temperature, rainfall, solar radiation, and sunlight duration, were used to evaluate the impact of climatic conditions on regional carbon storage and sequestration. (4) Socioeconomic data: Population, GDP, and nighttime light data were included to assess the impact of human activities and economic development on ecosystem carbon storage. Detailed information and specific data sources are provided in Table 1.

Table 1. Data preparation and data sources.

Data	Type	Scale	Year	Data Source
Landsat	Raster	30 m	1990, 2000, 2010, 2020	https://earthengine.google.com/ (accessed on 20 October 2023)
CLCD	Raster	30 m	1990–2020	https://zenodo.org/records/5210928 (accessed on 25 October 2023)
NDVI	Raster	1 km	1990–2020	https://data.tpdc.ac.cn/ (accessed on 23 March 2024)
Monthly NDVI	Raster	1 km	1990–1999	https://zenodo.org/record/6295928 (accessed on 27 March 2024)
	Raster	1 km	2000	https://www.resdc.cn/ (accessed on 27 March 2024)
	Raster	250 m	2001–2020	https://search.earthdata.nasa.gov/search (accessed on 27 March 2024)
MNDWI	Raster	1 km	1990, 2000, 2010, 2020	https://data.tpdc.ac.cn/ (accessed on 23 March 2024)
Population	Raster	1 km	1990, 2000, 2010, 2020	http://data.europa.eu/ (accessed on 23 March 2024)
Temperature	Raster	1 km	1990–2020	https://data.tpdc.ac.cn/ (accessed on 24 March 2024)
Rainfall	Raster	1 km	1990–2020	https://data.tpdc.ac.cn/ (accessed on 24 March 2024)
GDP	Raster	1 km	1990, 2000, 2010, 2020	https://www.resdc.cn/ (accessed on 25 March 2024)
DEM	Raster	30 m	-	http://www.resdc.cn/ (accessed on 25 March 2024)
Nighttime lighting	Raster	1 km	1990, 2000, 2010, 2020	https://data.tpdc.ac.cn/ (accessed on 25 March 2024)
Solar radiation	Raster	8 km	1990–2016	https://data.tpdc.ac.cn/ (accessed on 28 March 2024)
Sunshine hours	Digital	Monthly	1990–2020	Statistical Yearbook

2.2.2. Data Processing

(1) Extraction of Information on Wetland Types in the Coastal Zone

The random forest is an ensemble learning technique used for various tasks, including classification and regression. It operates by constructing a multitude of decision trees during training and then outputting the majority category (for classification) or the mean prediction (for regression) [40]. In this study, the decision tree model was built using a random sampling method, with 80% of the data serving as training samples and 20% as test samples. To classify wetland types in the coastal zone within the study area, we aggregated the votes from all decision trees and selected the category with the majority of votes as the final output [41].

Furthermore, utilizing the GEE platform, we applied the random forest algorithm to extract wetland data for the coastal zone of Jiaozhou Bay across different time periods. The wetlands were classified into four types: rivers, reservoirs, aquaculture ponds, and mudflats. In recent years, fishery carbon sinks have gained attention as the "missing carbon sink", becoming a significant component of marine blue carbon [42]. Aquaculture ponds were included in this study because Jiaozhou Bay is a renowned shellfish aquaculture base in China. To improve classification accuracy, we used all available spectral bands and six spectral indices as the basis for classification (Table 2). Additionally, we developed the Aquatic Reflectance Enhancement Index (AREI), specifically designed to enhance the accuracy and reliability of water body identification, thereby significantly improving the resolution of complex water features.

Table 2. Remote sensing indices used in the random forest algorithm.

Remote Sensing Index	Formulas	Description
$NDVI$	$NDVI = \frac{(NIR - Red)}{(NIR + Red)}$	The Normalized Difference Vegetation Index, which reflects crop growth status information.
$MNDWI$	$MNDWI = \frac{(Green - SWIR)}{(Green + SWIR)}$	The Modified Normalized Difference Water Index, which enhances the detection of water bodies.
EVI	$EVI = 2.5 \times \frac{(NIR - Red)}{(NIR + 6 \times Red - 7.5 \times Blue + 1)}$	The Enhanced Vegetation Index, which enhances vegetation signals and reduce atmospheric interference.
BSI	$BSI = \frac{(SWIR + Red) - (NIR + Blue)}{(SWIR + Red) + (NIR + Blue)}$	The Bare Soil Index, which identifies bare soil and urban areas.
IBI	$IBI = \frac{\left(2 \times \frac{SWIR1}{SWIR1 + NIR} - \left(\frac{NIR}{NIR + RED} + \frac{GREEN}{GREEN + SWIR1}\right)\right)}{\left(2 \times \frac{SWIR1}{SWIR1 + NIR} + \left(\frac{NIR}{NIR + RED} + \frac{GREEN}{GREEN + SWIR1}\right)\right)}$	The Index of Building Intensity, which identifies densely built-up areas.
$AREI$	$AREI = SWIR1 + TIR + MIR - Blue - Green - NIR$	The Aquatic Reflectance Enhancement Index, which improves the accuracy of water body identification.

(2) Construction of a Dataset to Fill Data Gaps Caused by Coastline Changes

Considering the potential impact of historical coastline changes on the dataset's coverage, this study specifically focused on new areas that may have been uncovered by recent activities such as land reclamation. By integrating 30 m resolution Landsat imagery from 2000 to 2020 with field research data and performing high-precision visual interpretation, we utilized the classification post-processing tool in ENVI software (version 5.6) to accurately fill in these uncovered or data-deficient areas. This process not only ensured the completeness of the dataset but also enhanced its utility for land use classification. Ultimately, we successfully constructed a land use map featuring nine types: rivers, reservoirs, aquaculture ponds, mudflats, croplands, forests, grasslands, bare lands, and built-up areas (Figure 3).

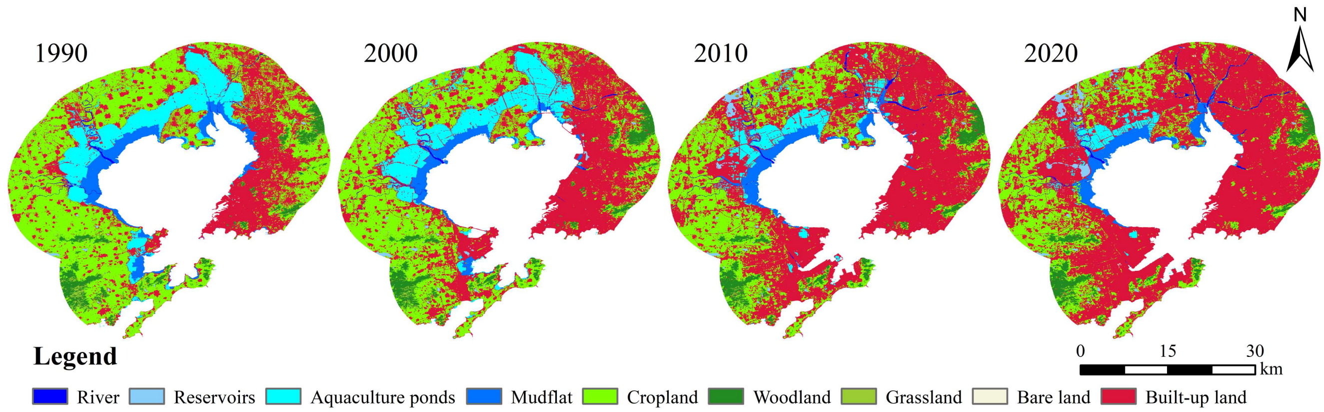

Figure 3. Land use types in Jiaozhou Bay (1990–2020).

2.3. Methods

This study integrates remote sensing data, land use data, and ecosystem service models to assess the spatiotemporal patterns of carbon storage and identify driving factors in the coastal zone of Jiaozhou Bay from 1990 to 2020. High-quality remote sensing data, such as Landsat imagery, have been available since 1990, making this period suitable for comprehensive analysis. Over these three decades, Jiaozhou Bay has undergone significant urban expansion and land use changes [36]. Additionally, this timeframe coincides with the availability of crucial socioeconomic data, such as GDP and population density, which are essential for a detailed analysis of the factors influencing carbon storage. By covering a 30-year period, this study aims to identify long-term trends and variations, providing valuable insights for sustainable land management and ecological protection strategies. This study employed InVEST model version 3.14.0 and GeoDetector version 2015.

2.3.1. InVEST Model

The InVEST model's carbon storage module is used to estimate the carbon storage and sequestration potential of different landscapes. This module quantifies carbon stored in various pools, including above-ground biomass, below-ground biomass, soil organic matter, and dead organic matter [40]. This study utilized the InVEST model to calculate changes in carbon storage in Jiaozhou Bay by using land use data and carbon density tables. The calculation of carbon storage is based on the following formula:

$$C_i = C_{i\_above} + C_{i\_below} + C_{i\_soil} + C_{i\_dead} \quad (1)$$

where C_i, C_{i_above}, C_{i_below}, C_{i_soil}, and C_{i_dead} denote the average carbon densities in megagrams per hectare (Mg/ha) for the total organic carbon pool, above-ground biomass, below-ground biomass, soil organic matter, and dead organic matter for the *i*-th land-use type, respectively. Parameter information is provided in the Supplementary Materials.

2.3.2. Improved CASA Model

The CASA model is a process-based remote sensing model used to estimate *NPP* and carbon sequestration services. It is advantageous due to its requirement for few input parameters, high data accessibility, and low error rates [43]. In this study, an improved CASA model [44] was employed, incorporating vegetation cover classification to enhance *NPP* estimation accuracy. The *NPP* calculation is based on the following formula:

$$NPP(x,t) = APAR(x,t) \times \varepsilon(x,\ t) \quad (2)$$

where $APAR(x,t)$ denotes the photosynthetically active radiation absorbed by pixel x in month t $\left(\mathrm{MJm^{-2}month^{-1}}\right)$, and $\varepsilon(x,t)$ denotes the actual light energy utilization of pixel x in month $\mathrm{t(gC/MJ)}$. The absorbed photosynthetically active radiation (APAR) is calculated using the following formula:

$$APAR(x,t) = SOL(x,t) \times FPAR(x,t) \times 0.5 \quad (3)$$

where $SOL(x,t)$ denotes the total solar radiation at pixel x in month t $\left(\mathrm{MJm^{-2}month^{-1}}\right)$, and $FPAR(x,t)$ is the fraction of incident photosynthetically active radiation absorbed by the vegetation layer [45].

Light energy utilization is influenced by the maximum light energy utilization ε_{max}, temperature, and precipitation [43]. It is calculated as follows:

$$\varepsilon(x,\ t) = T_{\varepsilon1}(x,\ t)\ \times T_{\varepsilon2}(x,\ t)\ \times W_{\varepsilon}(x,\ t)\ \times \varepsilon_{max} \quad (4)$$

where $T_{\varepsilon1}(x,\ t)$ and $T_{\varepsilon2}(x,\ t)$ represent the stress effects of low and high temperatures on light energy utilization, respectively; $W_{\varepsilon}(x,\ t)$ denotes the coefficient of moisture stress influence; and ε_{max} represents the maximum light energy utilization of vegetation under ideal conditions. Parameters values for different land use types are based on the existing studies and are shown in Table 3 [44].

Table 3. Maximum light use efficiency (ε_{max}) for different land use types.

land Use Type	Cropland	Forest	Shrub	Grassland	Water	Sonw/Ice	Bare Land	Impervious	Wetland
ε_{max}	0.542	0.389	0.429	0.542	0.542	0.542	0.542	0.542	0.542

Note: ε_{max} represents the maximum light use efficiency; all values are unitless.

Based on the CASA model for calculating NPP, the vegetation carbon sequestration model was used to estimate the annual carbon sequestration in Jiaozhou Bay. The calculation formula is as follows:

$$C = A \times k \times \sum_{i=1}^{n} NPP_i \tag{5}$$

where C denotes the total annual carbon sequestration (Mg/year) in the study area, NPP_i denotes the annual net primary productivity $\left(\text{gC/m}^2\text{/year}\right)$ of the i-th raster, A is the area of the raster, n is the total number of rasters, and k is the conversion coefficient between NPP and carbon sequestration.

2.3.3. Spatial Heterogeneity and Correlation Analysis Methods

GeoDetector is a statistical tool used to detect the spatial heterogeneity of geographical phenomena and their driving factors [46]. It is based on the fundamental assumption that if there is a significant correlation between an independent variable and a dependent variable, then these variables should exhibit similar spatial distributions [47,48]. The GeoDetector consists of four detectors: factor detector, interaction detector, risk detector, and ecological detector. In this study, the factor detector and interaction detector were used to explore the factors influencing the spatial distribution of carbon storage [49].

The factor detector uses the q-statistic to assess the explanatory power of each influencing factor on carbon storage. The q-statistic is calculated as follows:

$$q = 1 - \frac{\sum_{h=1}^{L} N_h \, \sigma_h^2}{N \, \sigma^2} \tag{6}$$

where q represents the explanatory power of the influencing factor on carbon storage; h h denotes the stratification of the influencing factor; N represents the total carbon storage in the entire region, and N_h represents the carbon storage within a specific stratum h; σ_h^2 and σ^2 represent the variance within stratum h and the entire study area, respectively. Larger q values indicate greater explanatory power [50].

Since the GeoDetector model requires discretized data, the resolution of different datasets was standardized, and factor variables were classified into six classes using the natural breakpoint method [46,49]. The Fishnet tool was used to generate numerical sampling points and extract the values of both the independent and dependent variables as input data for the GeoDetector model.

The interaction detector evaluates whether the interaction between two factors increases or decreases their explanatory power on the dependent variable [51]. By comparing the q-statistics of the factors detected individually and interactively, the assessment results can be categorized into five types. Table 4 presents the five categories of factor interactions [49].

Table 4. Interaction types of the factors driving the spatial differentiation of carbon storage.

Interaction Type	Judgment Criteria
Nonlinear attenuation	$q(X_1 \cap X_2) < \min[q(X_1),\, q(X_2)]$
Univariate nonlinear attenuation	$\min[q(X_1),\, q(X_2)] < q(X_1 \cap X_2) < \max[q(X_1), q(X_2)]$
Bivariate enhancement	$q(X_1 \cap X_2) > \max[q(X_1),\, q(X_2)]$
Nonlinear enhancement	$q(X_1 \cap X_2) > q(X_1) + q(X_2)$
Independent	$q(X_1 \cap X_2) = q(X_1) + q(X_2)$

Note: $X1$ and $X2$ are the influencing factors; $q(X1)$ and $q(X2)$ represent the influences of factors $X1$ and $X2$ on the spatial differentiation of carbon storage, respectively; $q(X1 \cap X2)$ represents the influence of the interaction between factors $X1$ and $X2$ on the spatial differentiation of carbon storage.

Pearson correlation analysis was also used to assess the linear relationships between different factors influencing carbon storage. Pearson correlation measures the strength and direction of the linear relationship between two continuous variables, with correlation coefficients ranging from −1 to 1. Positive coefficients indicate a direct relationship, while negative coefficients indicate an inverse relationship. This method complements the findings from GeoDetector [52].

3. Results

3.1. Characteristics of Spatial and Temporal Variations in Carbon Storage

In terms of total amount, the overall carbon storage in the coastal zone of Jiaozhou Bay exhibited a year-by-year decreasing trend from 1990 to 2020. The carbon storage decreased from 5.59×10^6 tC in 1990 to 4.62×10^6 tC in 2020, a reduction of 17%, totaling a decrease of 9.7×10^5 tC. Among these, the total carbon storage of wetland types decreased most significantly, from 4.66×10^5 tC in 1990 to 2.97×10^5 tC in 2020, a reduction of 36% (Figure 4). The decadal reduction rate of the total carbon storage in the coastal zone of Jiaozhou Bay gradually decreased, from 9.8% in 1990–2000 to 3.5% in 2010–2020. Further analysis reveals that the year 2000 marks a significant turning point. Taking 2000 as the boundary, the total carbon storage reduction in the first decade (1990–2000) was 1.3 times the total reduction in the following two decades (2000–2020). This indicates that the carbon storage decline was more severe in the earlier period, while the rate of decline moderated after the 21st century began.

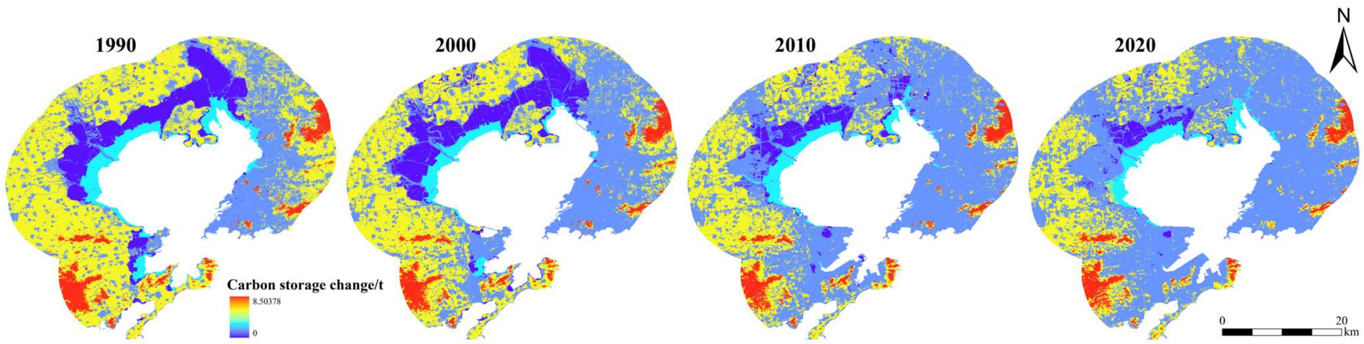

Figure 4. Change of carbon storage in Jiaozhou Bay (1990–2020).

In terms of the average annual rate of change, the average annual reduction in carbon storage was 5.50×10^4 tC in the period 1990–2000, 2.51×10^4 tC in the period 2000–2010, and 1.67×10^4 tC in the period 2010–2020. This indicates that the carbon storage decreased at the fastest rate in the first decade, while the rate of reduction significantly slowed in the later periods. Notably, in the period 2010–2020, the average annual reduction dropped to about one-third of the rate in the previous decade. Overall, both the total carbon storage in the coastal zone and the wetland carbon storage show a decreasing trend, but the rate of decrease is gradually narrowing, indicating a slowing trend in carbon loss.

In terms of spatial changes, the carbon storage in the coastal zone of Jiaozhou Bay exhibits significant spatial heterogeneity. The area along the bay is dominated by artificial land surfaces, heavily influenced by human activities. As a result, the carbon storage in this area remains low, classifying it as a low-carbon zone. From 1990 to 2020, the low-carbon zone expanded annually, spreading from the coastal area, gradually fragmenting and eroding the integrity of the high-carbon zones. This expansion caused a significant reduction in high-carbon zones, which retreated inland and became increasingly fragmented (Figure 4). Specifically, the high-carbon zones were distributed in patches and bands in the eastern and southwestern parts of the study area, located at relatively high elevations, mostly mountainous regions, with lush and diverse vegetation providing a rich source of soil organic carbon. The highest carbon density in these areas could reach 116.62 Mghm^{-2}. In contrast, the low-carbon areas were mainly distributed along the coast of Jiaozhou Bay, comprising built-up areas and aquaculture ponds, with the lowest carbon storage values at only 12.49 Mghm^{-2}. From the perspective of spatial pattern changes, the period from 1990 to 2000 saw significant shifts, primarily with medium–high-carbon areas transitioning to low-carbon areas in the eastern part of the study region, and the gradual loss of dominance of medium-carbon areas. From 2000 to 2010, the spatial pattern became further fragmented, with low-carbon areas surpassing medium-carbon areas for the first time and becoming the dominant type. Between 2010 and 2020, the spatial pattern stabilized, the rate of change slowed, and the ecological environment gradually stabilized. Overall, the carbon storage in the coastal zone of Jiaozhou Bay shows clear spatial differentiation characteristics. High-carbon areas are gradually decreasing and retreating inland, while low-carbon areas are expanding, fragmenting, and eroding the integrity of high-carbon areas, leading to their fragmentation. This trend reflects the dynamic and complex nature of the spatial distribution of carbon storage.

In terms of the trend of change, from 1990 to 2020, the carbon storage in the coastal zone of Jiaozhou Bay exhibited significant regional characteristics, characterized by large-scale aggregation and sporadic distribution. Among them, 74.13% of the areas had carbon storage that remained basically stable, 24.85% of the areas experienced significant decreases, and only 1.02% of the areas showed an increasing trend in carbon storage. The regions with significant decreases in carbon storage are widely distributed, mainly in noncoastal regions that have experienced dramatic urban expansion. In contrast, the areas with increasing carbon storage are smaller and scattered in the northern and western parts of the Jiaozhou Bay coastal zone. Carbon storage remains stable in most areas, especially in the coastal regions, which exhibit better integrity and stability. This suggests that in terms of the ecological environment, the coastal areas show strong stability (Figure 5).

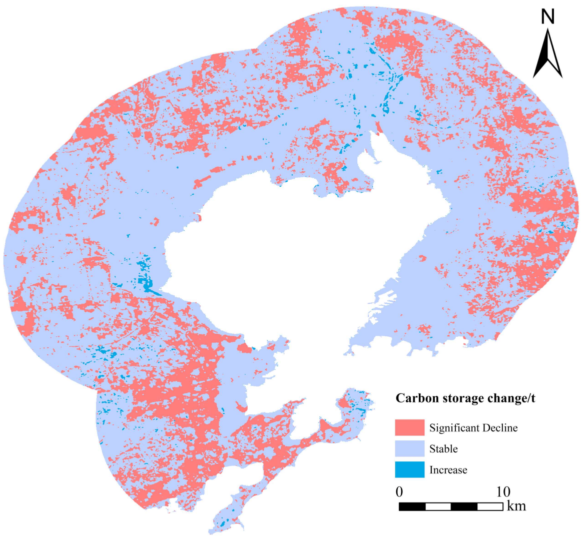

Figure 5. Carbon storage variations in Jiaozhou Bay (1990–2020).

3.2. Characteristics of Spatial and Temporal Variations in Carbon Sequestration

From 1990 to 2016, the annual carbon sequestration in the coastal zone of Jiaozhou Bay exhibited notable volatility and an overall downward trend. The annual carbon sequestration decreased from 203.56 Mg/year to 131.36 Mg/year, with significant interannual fluctuations during this period. Notably, the annual carbon sequestration peaked in 1992 at 242.02 Mg/year, which is 2.28 times the annual carbon sequestration in 2003. However, there was a marked decline after this peak, especially during the 1990s (Figure 6).

In terms of long-term trends, total annual carbon sequestration experienced a rapid decline from 1990 to 2000, falling from its peak to 110.45 Mg/year by 2000, almost halving. This dramatic decline indicates that environmental changes or human activities significantly impacted annual carbon sequestration levels during this decade. After this rapid decline, the drastic downward trend in annual carbon sequestration was effectively curbed. From 2000 to 2010, annual carbon sequestration fluctuated but remained relatively stable overall, with minor fluctuations, maintaining a range between 110 and 162 Mg/year. From 2010 to

2016, annual carbon sequestration continued to show minor fluctuations and a tendency to rebound, maintaining a range between 111 and 142 Mg/year. This indicates that the ecosystem's carbon sequestration capacity reached a relatively stable state with a rising trend during this period.

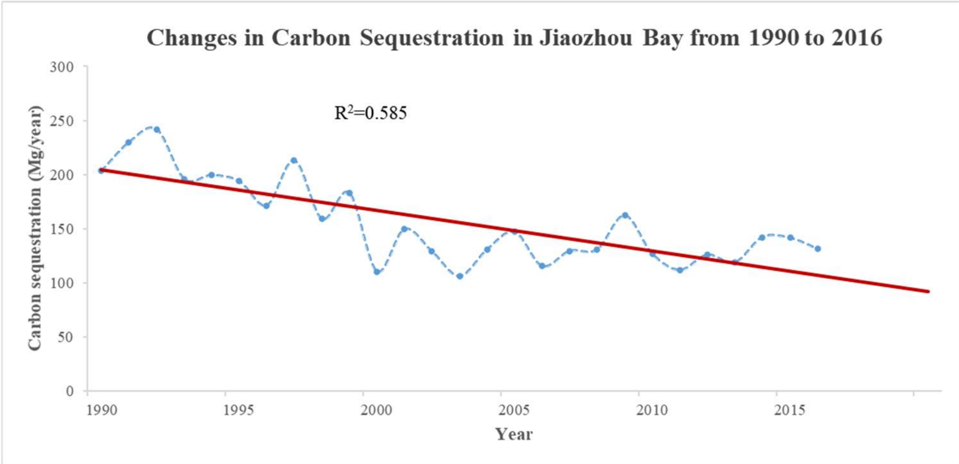

Figure 6. Carbon sequestration variations in Jiaozhou Bay (1990–2016).

In terms of the average annual rate of change, average annual carbon sequestration decreased by 9.31 Mg/year during the period 1990–2000, showing a clear downward trend. However, during the period 2010–2016, the average annual carbon sequestration increased slightly by 0.46 Mg/year. This indicates that, after a drastic decrease in the 1990s, the annual carbon sequestration of the vegetation in the coastal zone of Jiaozhou Bay gradually stabilized and showed a slow rebound in the 21st century. This trend suggests that the carbon sequestration capacity of the ecosystem has gradually recovered after the initial sharp decline and has made some progress in recent years. This rebound also reflects the effectiveness of ecological protection measures, indicating that the implementation of environmental management and protection efforts has positively impacted the carbon sequestration capacity of ecosystems during this period.

In terms of spatial changes, the Mann–Kendall test results (Figure 7) indicate that in the coastal zone of Jiaozhou Bay, the annual carbon sequestration remained relatively stable in most areas, with no significant changes in about 68.0% of the areas. However, about 32.0% of the areas showed a significant decreasing trend in annual carbon sequestration. These areas with significant decreases are mainly concentrated in the northern part of the coastal zone, which is relatively flat and has experienced the most drastic urban expansion. Additionally, some areas with decreasing annual carbon sequestration are sporadically distributed throughout the study area. The areas where annual carbon sequestration remained relatively stable are spread throughout the entire coastal zone of Jiaozhou Bay, particularly concentrated on the west and east coasts. However, these two shores exhibit completely different development patterns: the west coast has maintained a relatively good natural ecological environment with relatively little urban expansion during the social development from 1990 to 2020, while the east coast has been under high-intensity development with a very high urbanization rate during this 30-year period. Further analysis revealed that 49.0% of the areas with significant decreases in annual carbon sequestration were located in urban expansion areas. This indicates that the urbanization process has significantly impacted the ecological environment of the coastal zone of Jiaozhou Bay, reducing its carbon sequestration capacity. Overall, although annual carbon sequestration remained stable in most areas, the negative impacts of land use change and ecological damage caused by urbanization on annual carbon sequestration should not be ignored.

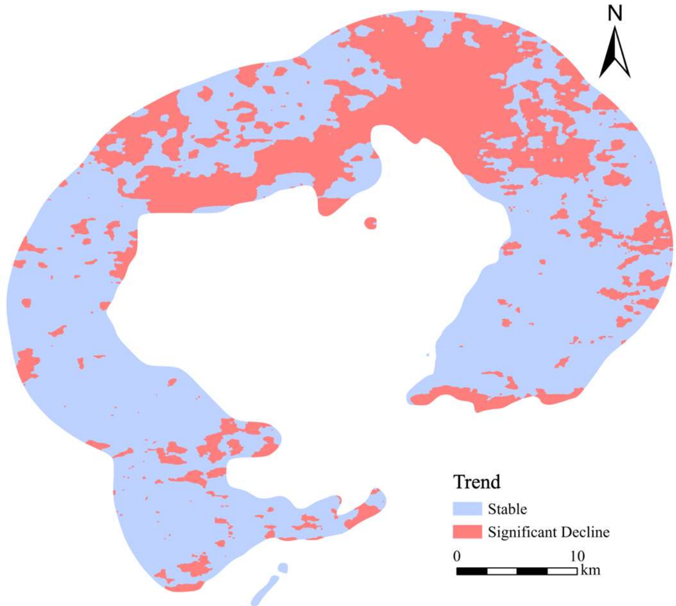

Figure 7. M–K test results for carbon sequestration (1990–2016).

4. Discussion

4.1. Factors Affecting Carbon

The factors affecting carbon storage in the coastal zone are variable and complex, and studies have shown that natural environmental factors and human activities exert varying degrees of influence on coastal carbon storage [53]. In this study, nine natural environmental factors and four socioeconomic factors were selected for in-depth analysis. These natural environmental factors include elevation (DEM), distance from the coast (Dco), Modified Normalized Difference Water Index (MNDWI), Normalized Difference Vegetation Index (NDVI), mean annual precipitation (Prec), slope (Slp), mean annual temperature (Temp), extreme climate (EC), and temperature range (TR). The socioeconomic factors include gross domestic product (GDP), night light index (NL), population density (PD), and industrial structure (IS). Among these factors, temperature range (TR) indicates the difference between the monthly average temperatures of the hottest and coldest months of the year, while extreme climate (EC) reflects the difference between the highest and lowest temperatures recorded during the year.

GeoDetector and Pearson correlation analysis are both valuable tools for analyzing the factors influencing carbon storage, but they have distinct strengths and applications. GeoDetector excels in detecting spatial heterogeneity and the interactions between factors, making it highly effective for understanding the complex spatial patterns of carbon storage. It quantifies the explanatory power of each factor and their interactions, which is particularly useful for spatially stratified phenomena.

On the other hand, Pearson correlation analysis measures the strength and direction of linear relationships between continuous variables. It provides a straightforward method to assess the correlations between factors influencing carbon storage. Pearson correlation is easy to compute and interpret, making it suitable for initial exploratory analysis to identify potential linear relationships between variables.

The results of this study (Table 5, Figures 8 and 9) show significant differences in the explanatory power of various drivers on carbon storage changes. The *p*-values for all detected factors were less than 0.01, confirming their statistical significance. Among them, NDVI exhibited the highest q-statistic value of 0.289, making it the dominant factor in the region. This underscores the crucial role of vegetation cover in carbon sequestration capacity, as vegetation fixes carbon dioxide in biomass through photosynthesis. Higher NDVI values indicate dense vegetation and strong carbon sequestration capacity. Therefore, the higher the NDVI value, the greater the carbon storage. Pearson correlation analysis supports this, showing a strong positive correlation between NDVI and carbon storage (r = 0.453 to 0.564 across different years). Vegetation not only absorbs and stores carbon but also increases the organic carbon content in the soil through roots and litter, maintaining the carbon balance of the ecosystem. Studies have shown that wetlands, such as mangroves, swamps, and marshes, store significantly more carbon compared to other ecosystems due to their dense vegetation and biomass. For instance, Mexican wetlands have been documented to store 13, 7, 6, and 5 times more carbon than terrestrial ecosystems [54].

Table 5. Explanatory power (q) and significance (*p*) of single factors for carbon storage.

Factors	DEM	Dco	GDP	NL	MNDWI	NDVI	PD	Prec	Slp	Temp	IS	EC	TR
q-statistics	0.032	0.030	0.120	0.082	0.235	0.289	0.075	0.040	0.018	0.079	0.099	0.089	0.040
p-value	0	0	0	0	0	0	0	0	0	0	0	0	0

Note: Dco indicates distance from coast; NL represents nighttime light; PD measures population density; Prec quantifies precipitation; Slp denotes slope; Temp reflects temperature; IS indicates industrial structure; EC measures extreme climate, and TR captures temperature range.

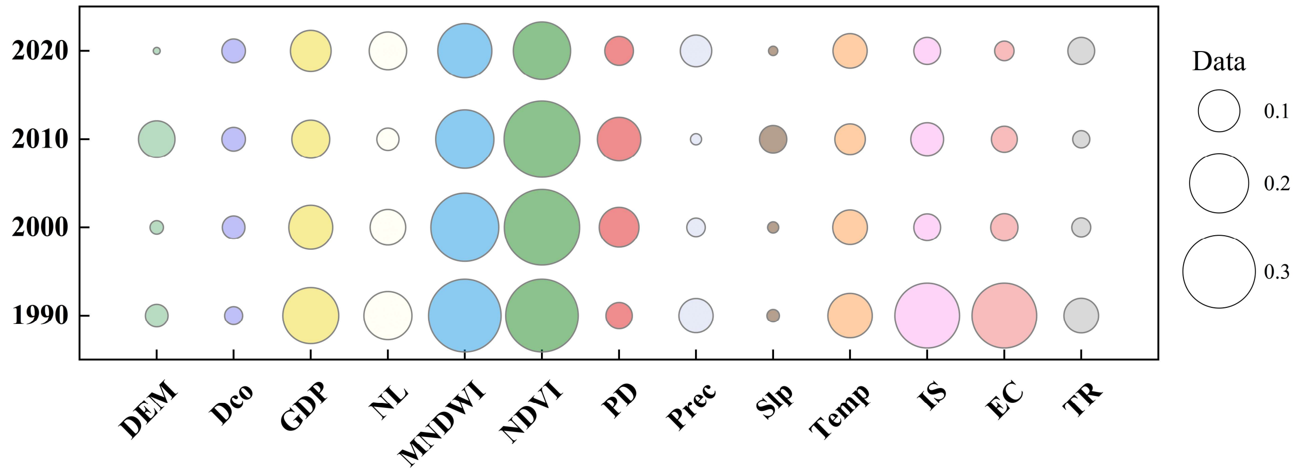

Figure 8. Explanatory power of single factors for carbon storage.

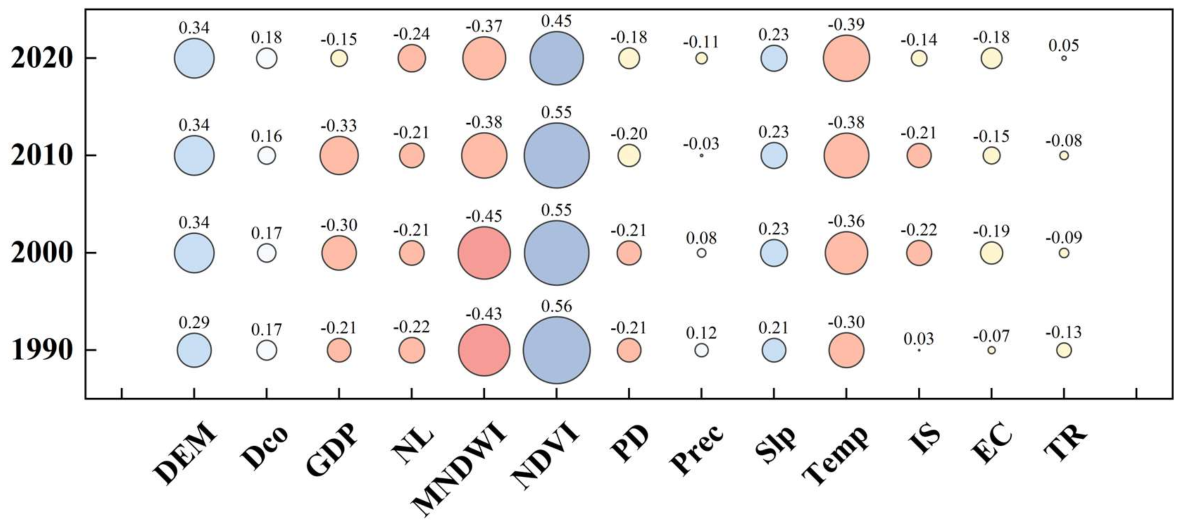

Figure 9. Pearson correlation coefficients between carbon storage and influencing factors: Bubble size represents correlation strength, red indicates negative correlations, and blue indicates positive correlations.

Second, MNDWI also had a significant effect on carbon storage, reflecting the importance of moisture conditions on ecosystem carbon storage. The MNDWI indicates the distribution of water in the region. Good water conditions are crucial not only for vegetation growth and increased coverage but also for supporting microbial activity, which accelerates organic matter decomposition and soil carbon formation. Pearson correlation analysis indicates a negative correlation between MNDWI and carbon storage ($r = -0.434$ to -0.366), suggesting that while good moisture conditions support carbon storage, excessive water might negatively impact it through other means.

Natural factors such as Temp, EC, and TR affect the temperature conditions for plant growth and climate stability, respectively. Suitable temperature conditions not only contribute to the prosperity of vegetation and carbon fixation but also promote carbon cycling in ecosystems. Extreme climates and large temperature ranges reflect climate stability; frequent extreme climates and large temperature differences may lead to ecosystem degradation, thus affecting the carbon sequestration efficiency of vegetation and the stability of carbon storage [55,56]. Pearson correlation analysis shows negative correlations for Temp ($r = -0.3$ to -0.392), EC ($r = -0.070$ to -0.184), and TR ($r = -0.132$ to 0.048), indicating that higher temperatures and climate extremes negatively impact carbon storage.

Although the explanatory power of anthropogenic indicators such as GDP, PD, and NL is relatively low, it remains significant. Among the anthropogenic factors, GDP has the highest explanatory power, reflecting the intensity of economic and human activities, including urbanization, industrial development, and infrastructure construction. These factors have complex impacts on the formation and alteration of carbon storage in the coastal zone. Economic development is usually accompanied by land use changes, such as wetland degradation and urban expansion, which are associated with significant carbon exchange and loss. Pearson correlation analysis indicates a negative correlation between GDP and carbon storage ($r = -0.205$ to -0.147), supporting the notion that increased economic activity may reduce carbon storage. Social activities promoting the sustainable development of a green economy can also contribute to increasing carbon storage. The NL and PD are also indicators of human activities. The difference is that NL reflects the intensity of human activities, while PD reflects their concentration. In urbanized and industrialized areas, higher NL values indicate frequent human activity, often accompanied by reduced vegetation cover and increased soil erosion, which in turn affects carbon fixation and storage. Similarly, high population density is often accompanied by land development and construction activities, leading to reduced vegetation cover and ecosystem destruction, resulting in a decline in carbon storage. Correlation analysis supports these observations with negative correlations for NL ($r = -0.22$ to -0.239) and PD ($r = -0.205$ to -0.182). The interaction between natural and socioeconomic factors plays a crucial role in carbon storage. These interactions often result in nonlinear and synergistic effects that are more significant than the sum of individual factors [54]. Economic activities, indicated by factors such as GDP, population density, and night light, have complex impacts on carbon storage. While economic development can lead to land use changes and reduced vegetation cover, sustainable development practices can help mitigate these effects and enhance carbon storage [57].

The average explanatory power of natural and socioeconomic factors was 9.46% and 9.38%, respectively, revealing the combined influence of natural and anthropogenic factors on the spatial distribution of carbon storage in the coastal zone of Jiaozhou Bay. In general, vegetation cover and moisture conditions are the main natural factors affecting carbon storage, while the combined influence of socioeconomic factors should not be overlooked despite their lower individual explanatory power. By analyzing these driving factors and the mechanisms behind them in depth, we can better understand the changing patterns of carbon storage and provide a scientific basis for the formulation of effective carbon management and ecological protection policies.

In this study, the selected factors were interactively probed, and all interactions were enhanced, indicating that the interaction between factors affects the spatial differentiation of carbon storage in a nonlinear and bifactorial manner. The complex coupling between different factors influences the spatial differentiation of carbon storage, with 34 nonlinear enhancements and 44 bivariate enhancements identified (Figure 10b).

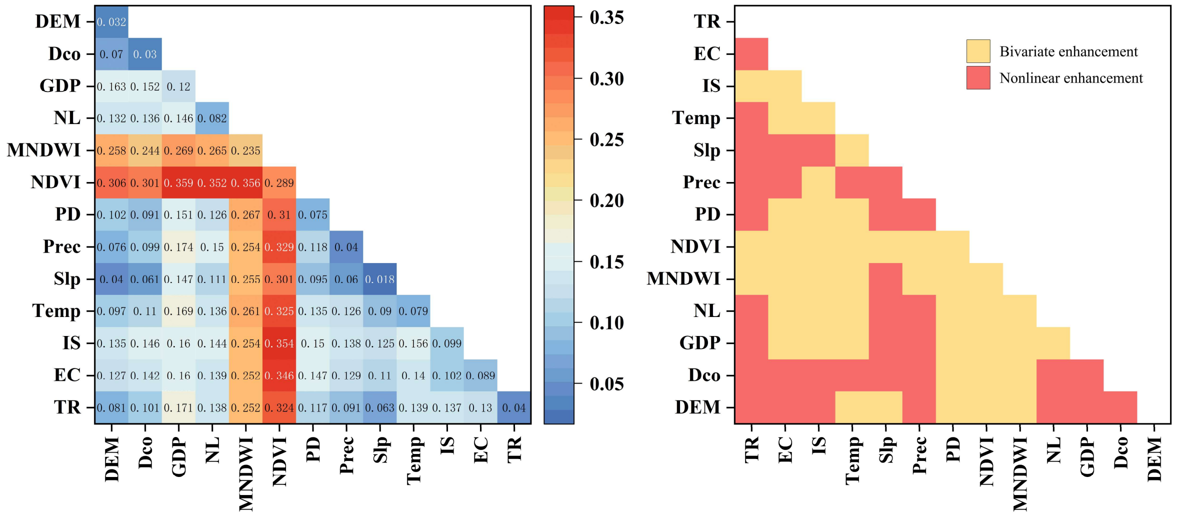

(**a**) (**b**)

Figure 10. (**a**) Explanatory power of multifactor interaction detection (q); (**b**) type of interaction detection, where red indicates nonlinear enhancement and yellow represents bivariate enhancement.

The results of this study (Figure 10a) show that the interaction between NDVI and GDP in the coastal zone of Jiaozhou Bay produced the combination with the strongest explanatory power for carbon storage in the study area, with a q-statistic value of 0.359. This can be understood as changes in NDVI simultaneously enhancing the explanatory power of GDP for regional changes in carbon storage. From 1990 to 2020, driven by economic development, the urbanization rate in the coastal zone of Jiaozhou Bay increased from 29.83% to 64.66%. Land use changes led to a decrease in vegetation cover from 50.35% to 25.97%, which in turn affected the carbon storage in the study area. Additionally, the interactions of NDVI, MNDWI, and GDP with other factors also yielded high q-statistic values.

This result suggests that the ecosystem of the coastal zone of Jiaozhou Bay is influenced by the interaction of multiple factors, not simply by addition or independence, but through nonlinear and bivariate enhancements. For example, the combination of vegetation cover (NDVI) and economic activity (GDP) not only increases land use changes but also further affects carbon storage by altering ecosystem structure and function. Additionally, the interaction of moisture conditions (MNDWI) and vegetation cover also showed significant effects. This interaction may affect carbon fixation and storage by influencing plant growth and water use efficiency.

Such complex interaction mechanisms indicate that the effects of a single factor are often amplified or altered in multifactor interactions, creating new ecological effects. For example, in regions experiencing rapid economic development, even with high vegetation cover, the carbon sequestration capacity of vegetation can be limited if water resources are scarce. Similarly, in the context of climate change, changes in temperature and precipitation, by affecting plant growth and soil moisture, can act in conjunction with socioeconomic factors to alter the distribution and trends in carbon storage.

Overall, carbon storage in the coastal zone of Jiaozhou Bay is influenced by the complex coupling of natural and anthropogenic factors. This nonlinear enhancement and two-factor enhancement effect emphasizes the importance of considering the combined effects of multiple factors in ecosystem management. Understanding these interaction mechanisms can help formulate more effective carbon management and ecological protection policies, thereby better addressing the challenges of climate change and ecosystem change.

4.2. Analysis of Factors Influencing Carbon Storage

4.2.1. Analysis of the Impact of LUCC on Carbon Storage

LUCC is one of the key factors affecting ecosystem carbon sequestration services [58]. Converting cropland or wetlands to built-up areas can destroy soil and vegetation, releasing large amounts of CO_2 into the atmosphere, thereby reducing the carbon sequestration capacity of ecosystems. Additionally, the conversion of natural ecosystems to agricultural ecosystems significantly reduces the soil's carbon storage capacity [16,17]. For example, converting forests and grasslands to agricultural land, or wetlands to agricultural land, disturbs the soil and vegetation, resulting in the loss of carbon storage and nutrients [59].

According to the results of this study (Figures 4 and 11), the conversion of land use types in the study area led to significant changes in carbon storage. From 1990 to 2020, land use types in the coastal zone of Jiaozhou Bay changed significantly. The expansion of built-up land and the substantial decrease in the cropland and aquaculture ponds were particularly prominent. The built-up land increased by 410.40 km^2, primarily due to the decrease in the area of cropland and aquaculture ponds. Cropland decreased by 248.21 km^2, especially between 2000 and 2010, and the area of aquaculture ponds decreased by 85.49 km^2. This study showed that the reduction in the area of cropland and woodland led to significant carbon storage loss, accounting for 86.98% and 5.33% of the total carbon storage loss, respectively, while the conversion of aquaculture ponds to built-up land contributed to 60.75% of the increase in carbon storage. The average contributions of different land use types to the total carbon storage in the study area, in descending order, were cropland, built-up land, woodland, mudflat, aquaculture pond, grassland, reservoirs, river, and bare land. Notably, cropland was the largest contributor to carbon storage in the coastal zone of Jiaozhou Bay between 1990 and 2010. However, by 2020, built-up land surpassed cropland as the top contributor to carbon storage. This is mainly due to the continuous expansion of built-up land encroaching on cropland from 1990 to 2020, leading to a continuous decline in cropland carbon storage and a continuous increase in the carbon storage contribution of built-up land. Despite the lower carbon density of built-up land, their carbon storage contribution value rose to the top position because they occupy the highest absolute share in the study area. The combined average total carbon sequestration of cropland and built-up land accounted for 80.49% of the total carbon sequestration in the coastal zone of Jiaozhou Bay.

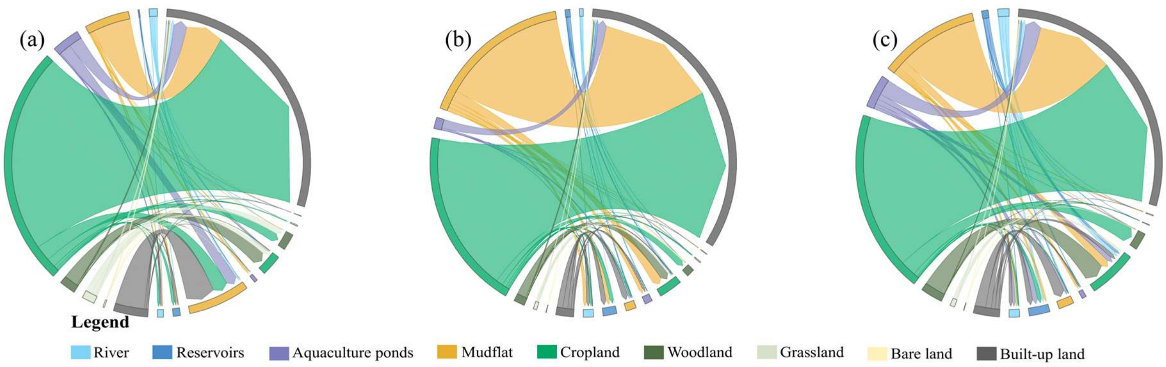

Figure 11. Transfer matrix of land use per decade in Jiaozhou Bay (1990–2020). (**a**) Transfer matrix of land use during 1990–2000; (**b**) transfer matrix of land use during 2000–2010; (**c**) transfer matrix of land use during 2010–2020.

In addition to cropland and built-up land, which occupy the largest share of the area, woodlands and mudflats, although smaller in area, make significant contributions to the carbon storage in the coastal zone of Jiaozhou Bay due to their higher carbon density values. Despite the small total area of reservoirs, their contribution to carbon storage rose from seventh to fifth, highlighting their increasing importance in the coastal zone ecosystem of Jiaozhou Bay. This increase is due to the creation of many artificial reservoirs between 1990 and 2020, which expanded their area and, thus, significantly increased their contribution to carbon storage. Furthermore, natural ecosystems such as rivers, woodlands, and grasslands also underwent significant changes during these 30 years, with approximately 13.2% of these natural ecosystems (including rivers, reservoirs, mudflats, woodlands, and grasslands) being converted into cropland, leading to a loss of soil carbon (Figure 11).

Overall, land use changes in the study area have had a profound impact on carbon storage. Cropland and built-up land dominate the carbon storage contribution, while other types such as woodland, mudflats, and reservoirs, although smaller in area, still contribute significantly to the regional carbon storage due to their high carbon density. This study shows that rational planning of land use is crucial for enhancing the carbon sequestration capacity of ecosystems.

4.2.2. Impact of Climate on Carbon Storage

Climate factors significantly influence the spatiotemporal distribution of carbon storage in coastal zones. Climate affects hydrothermal conditions, which in turn influence the decomposition rate of vegetation litter, ultimately impacting soil organic carbon content.

GeoDetector results indicate that climate factors, especially temperature, have a substantial impact on carbon storage in coastal zones (Figure 8). This finding is corroborated by Pearson correlation analysis. Temperature shows a moderate explanatory power (q-statistic = 0.073 to 0.116), and Pearson correlation analysis reveals a negative correlation between temperature and carbon storage ($r = -0.3$ to -0.392) (Figure 9). This suggests that rising temperatures negatively affect carbon storage, likely due to limitations on vegetation growth and increased soil microbial respiration caused by higher temperatures, leading to a reduction in carbon storage.

Furthermore, precipitation and its spatial distribution also influence carbon storage to some extent. Pearson correlation analysis shows that precipitation and carbon storage can be both positively and negatively correlated, indicating that while adequate moisture conditions support vegetation growth and carbon storage, excessive rainfall can lead to waterlogging, negatively impacting soil structure and microbial activity, and thereby reducing carbon storage.

Extreme climate events and temperature range also have significant explanatory power regarding carbon storage. Generally, both EC and TR show a negative correlation with carbon storage, indicating that extreme temperatures and temperature fluctuations can destabilize carbon storage. GeoDetector results confirm these findings, with extreme climate events and temperature range showing moderate explanatory power.

4.2.3. Impact of Economic Factors on Carbon Storage

Based on Pearson correlation analysis, GDP, NL, and PD all show negative correlations with carbon storage. An increase in GDP typically indicates heightened industrial activities, urban expansion, and infrastructure development, all of which involve significant land use changes. The night light index serves as a proxy for human activity intensity and is highly correlated with population density.

From 1990 to 2020, the expansion of built-up areas was a major trend in the region (Figure 11), leading to substantial vegetation loss and soil carbon depletion. Similarly, areas with high human activity density often exhibit lower carbon storage due to land use changes and habitat destruction, negatively impacting carbon storage.

GeoDetector results confirm the significant impact of economic factors and human activities on carbon storage (Figure 8). These findings underscore the importance of considering economic growth and human activity in carbon management strategies.

In conclusion, economic factors significantly impact carbon storage in coastal ecosystems. Sustainable economic growth, efficient land use planning, and conservation policies are essential to enhance carbon storage and maintain ecological balance in coastal zones.

4.3. Comparison of InVEST and Improved CASA Models

NPP is the net amount of carbon dioxide fixed by plants through photosynthesis minus the carbon released by respiration [60]. It is a sensitive indicator of climate and environmental change and is closely related to carbon storage. The magnitude of *NPP* directly determines the rate of carbon sequestration by plants, thus affecting the carbon storage capacity of ecosystems. In this study, we calculated the carbon storage and annual *NPP* of the coastal zone of Jiaozhou Bay from 1990 to 2020 and from 1990 to 2016, respectively, using the InVEST model and the improved CASA model, and converted the annual *NPP* to carbon sequestration.

The results showed that the trends of carbon storage changes and annual carbon sequestration in Jiaozhou Bay were similar, and the trends and spatial distribution of carbon storage and sequestration were highly consistent, indicating a strong correlation between ecosystem productivity and carbon storage in the coastal zone of Jiaozhou Bay. Under the pressure of environmental changes and human activities, the health of the ecosystem continues to deteriorate. From 1990 to 2020, the carbon storage showed a decreasing trend, with the rate of decline gradually decreasing. Although the data on annual carbon sequestration only cover the period from 1990 to 2016, the decreasing trend is consistent with the change in carbon storage. This pattern coincides with the change in cultivated land area in Qingdao, which decreased from 102 km^2 per decade to 52 km^2 per decade during the same period. This shows that the region has transitioned from rapid urbanization, which led to the encroachment of a large amount of arable land, and to the implementation of the "Protect the Bay and Develop around the Bay" strategy by Qingdao in 2007, aimed at protecting the ecological environment. In recent years, conservation measures in the coastal zone of Jiaozhou Bay have achieved remarkable results, and the trends in carbon storage and annual carbon sequestration indicate that the ecological environment is stabilizing.

Although both the InVEST model and the improved CASA model are based on LUCC data, there are significant differences in modeling principles and applications. The InVEST model excels at comprehensively assessing ecosystem carbon sequestration capacity by quantifying the carbon in various carbon pools. However, its accuracy depends on exhaustive carbon pool data, and it has a limited ability to reflect the complexity of ecosystem carbon sequestration mechanisms. In contrast, the CASA model, as a process-based remote sensing model, has advantages in data availability and parameter inputs, but its ability to accurately estimate carbon sequestration in small areas is weaker, particularly due to its high requirements for accuracy in land use classification and parameters [61,62]. Therefore, for estimating carbon storage and annual carbon sequestration in small areas, more mature ecosystem service valuation models like the InVEST model may provide more accurate results than the CASA model, better reflecting the region's carbon storage and productivity.

Comparing Figures 5 and 7, it can be seen that both the distribution of carbon storage changes calculated using the InVEST model and the distribution of carbon sequestration changes calculated using the CASA model show that the vast majority of the area remained relatively stable, with a small portion experiencing significant decreases in carbon storage and sequestration, and only 1% showing an increasing trend in carbon storage. This spatial pattern indicates that the carbon sequestration capacity of the coastal zone ecosystem in Jiaozhou Bay is experiencing a rapid decline. Further analysis revealed that areas with declining carbon storage and sequestration were mainly concentrated in zones with drastic urbanization and land use changes. Especially in areas with frequent urban expansion, industrial development, and agricultural activities, these human activities have led to significant vegetation destruction and soil carbon loss, thereby markedly reducing the carbon storage capacity and ecosystem service function of the region. Overall, the decline in carbon storage and sequestration capacity in the coastal zone of Jiaozhou Bay reflects serious challenges facing the regional ecosystem. To reverse this trend, there is an urgent need to strengthen the ecological protection and restoration efforts in the Jiaozhou Bay coastal zone.

4.4. Limitations of This Study and Future Directions

Within the context of this study, the following limitations should be pointed out and could be further explored in future studies. First, there may be some uncertainties in the remote sensing data and other datasets used in this study due to data availability and resolution limitations. For example, the calculation of annual carbon sequestration was limited to 1990–2016 due to the lack of solar radiation data from 2017–2020. Additionally, errors might be present in the calculation of annual carbon sequestration because the monthly NDVI data were obtained from three different sources. Furthermore, although the random forest and CASA models showed relatively good classification and estimation in this study, the accuracy and generalization ability of the models were constrained by data quality. It should also be noted that, although GeoDetector can reveal the relationships and interactions between carbon storage and the influencing factors, it is limited in the ability to explore complex nonlinear relationships and spatiotemporal distributions.

Another significant limitation of this study arises from the dynamic nature of the coastline in the Jiaozhou Bay area. Over the years, natural processes such as erosion, sediment deposition, and sea-level rise, along with anthropogenic activities like land reclamation and infrastructure development, have led to changes in the coastline. Consequently, the shape and area of the study region have experienced slight variations over time. For instance, the study area was initially determined based on the 1990 coastline and extended 10 km inland. The study areas for 2000, 2010, and 2020 were determined by combining the land boundary of the 1990 study area with the coastline of each respective year. These adjustments in the study area's boundaries lead to minor variations in the total area covered each year. This results in the carbon storage calculations not being strictly based on the same area, introducing an element of uncertainty in the total carbon storage estimates.

Future research will focus on the following aspects: First, with the continuous development and advancement of remote sensing and geographic information, datasets with higher spatial and temporal resolution should be used to improve the accuracy and reliability of the research. Second, more advanced machine learning algorithms and ecological assessment models should be explored to enhance the accuracy of land use classification and carbon storage estimation. Additionally, a deeper investigation into the mechanisms affecting ecological changes and carbon storage dynamics, especially the combined effects of socioeconomic development and climate change on coastal carbon storage, will better aid in assessing and predicting the trends of spatiotemporal changes in carbon storage. Finally, emphasis should be placed on researching ecosystem restoration and management strategies, evaluating the impacts of various conservation measures on ecosystem health and carbon storage, thereby providing a basis for the formulation of more effective ecological protection policies.

5. Conclusions

This study, leveraging remote sensing data, employs the InVEST model and CASA model to conduct a comprehensive quantitative analysis of carbon storage and annual carbon sequestration in the coastal zone of Jiaozhou Bay from 1990 to 2020. By evaluating the spatial and temporal changes in these parameters, this study uncovers the driving factors behind these variations and provides crucial insights for the sustainable development and ecological protection of Jiaozhou Bay. The key conclusions drawn from this research are as follows:

(1) From 1990 to 2020, carbon storage and annual carbon sequestration in the coastal zone of Jiaozhou Bay experienced a notable decline, which has shown signs of stabilization in recent years. This trend underscores the profound impact of urbanization on land use patterns, transitioning from a focus on rapid economic development to prioritizing ecological protection. This study highlights the critical role of vegetation cover (NDVI) and water bodies (MNDWI) in regional carbon storage, emphasizing the need to maintain ecological integrity for effective carbon sequestration. Policymakers are increasingly integrating environmental considerations into economic development decisions, aiming to strike a balance

between growth and sustainability. Socioeconomic factors such as GDP and population density (PD), though less directly impactful on carbon storage, significantly influence land use patterns and carbon storage dynamics.

(2) Over the past three decades, Jiaozhou Bay has seen substantial land use changes, particularly an increase in built-up areas and a decrease in cultivated land and wetlands. The proportion of built-up areas surged from 29.83% to 64.66%, encroaching on croplands and wetlands, key sources of carbon storage. These changes highlight the immense pressure from human activities on the ecological service system. Government agencies must address the conflict between economic development and ecological protection, particularly in rapidly urbanizing areas, by protecting high-value carbon storage regions and rationalizing land use spatial layouts.

(3) Model comparison and integration: The comparison between the InVEST and CASA models reveals a high degree of consistency in the spatial and temporal trends of carbon storage and annual carbon sequestration. The InVEST model excels in quantifying carbon in various pools, providing detailed insights into an ecosystem's carbon sequestration capacity. In contrast, the CASA model offers high-precision ecosystem productivity assessments using remote sensing technology. The integration of these models enhances the accuracy and reliability of carbon storage assessments, offering robust data support for ecosystem management and policy formulation. Future research should continue to refine the integrated application of these models to further enhance the credibility of ecosystem carbon storage assessments.

(4) This study underscores the necessity of comprehensive land remediation, which requires balancing ecological and economic considerations. Policymakers should prioritize the establishment of protected areas in regions with high carbon storage potential to prevent further degradation and promote natural carbon sequestration processes. Land use planning policies should integrate carbon storage considerations, restricting urban expansion in high-carbon areas and promoting green infrastructure in urban environments. Economic incentives, such as payments for ecosystem services (PES), tax breaks, or subsidies for sustainable agricultural practices, should be introduced to encourage conservation and restoration activities. Establishing robust monitoring and evaluation frameworks is crucial for tracking the effectiveness of land remediation strategies. By implementing these targeted actions, policymakers can enhance the resilience of coastal zones, promote sustainable development, and achieve a harmonious balance between environmental protection and economic growth.

In conclusion, the findings of this study highlight the intricate relationship between land use changes, human activities, and carbon storage dynamics in coastal zones. By adopting a holistic approach to land management and policy formulation, it is possible to enhance regional carbon storage capacity, contribute to global climate goals, and ensure sustainable development for future generations.

Supplementary Materials: The following supporting information can be downloaded at: https://www.mdpi.com/article/10.3390/land13081208/s1, Table S1: Carbon density of Jiaozhou Bay (Mg/hm^2); references [20,63–69] are cited in the Supplementary Materials.

Author Contributions: Conceptualization, Q.G.; methodology, Q.G. and L.Z.; software, L.Z.; validation, Q.G.; formal analysis, L.Z.; investigation, L.Z.; resources, Q.G.; data curation, L.Z. and X.Z.; writing—original draft preparation, L.Z.; writing—review and editing, Q.G.; visualization, L.Z., H.L., J.C. and T.M.; supervision, Q.G.; project administration, Q.G.; funding acquisition, Q.G. All authors have read and agreed to the published version of the manuscript.

Funding: This research was funded by the National Natural Science Foundation of China (grant number 42106215), the Natural Science Foundation of Shandong Province, China (grant number ZR2021QD064), and Fundamental Research Funds for the Central Universities (grant number 22CX06033A).

Data Availability Statement: The original contributions presented in this study are included in the article and Supplementary Materials, further inquiries can be directed to the corresponding author.

Conflicts of Interest: The authors declare no conflicts of interest. The funders had no role in the design of the study; in the collection, analyses, or interpretation of data; in the writing of the manuscript; or in the decision to publish the results.

Abbreviations

The following abbreviations are used in this manuscript:

LUCC	Land use and cover change
CASA	Carnegie Ames Stanford Approach
NEP	Net ecosystem productivity
LPJmL	Lund–Potsdam–Jena Managed Land model
InVEST	Integrated Valuation of Ecosystem Services and Trade-offs model
NPP	Net primary productivity
CLCD	Annual China Land Cover Dataset
AREI	Aquatic Reflectance Enhancement Index
GEE	Google Earth Engine
NDVI	Normalized Difference Vegetation Index
DEM	Digital elevation model
MNDWI	Modified Normalized Difference Water Index
EVI	Enhanced Vegetation Index
BSI	Bare Soil Index
IBI	Index of building intensity
APAR	Absorbed photosynthetically active radiation
FPAR	Fraction of photosynthetically active radiation
SOL	Total solar radiation
Dco	Distance from the coast
Prec	Mean annual precipitation
Slp	Slope
Temp	Mean annual temperature
EC	Extreme climate
TR	Temperature range
GDP	Gross domestic product
NL	Night light index
PD	Population density
IS	Industrial structure

References

1. Macreadie, P.I.; Anton, A.; Raven, J.A.; Beaumont, N.; Connolly, R.M.; Friess, D.A.; Kelleway, J.J.; Kennedy, H.; Kuwae, T.; Lavery, P.S. The future of Blue Carbon science. *Nat. Commun.* **2019**, *10*, 3998. [CrossRef] [PubMed]
2. Dahl, T.E. *Status and Trends of Wetlands in the Conterminous United States 2004 to 2009*; Department of the Interior, Fish and Wildlife Service: Washington, DC, USA, 2011; 108p.
3. Costanza, R.; d'Arge, R.; De Groot, R.; Farber, S.; Grasso, M.; Hannon, B.; Limburg, K.; Naeem, S.; O'neill, R.V.; Paruelo, J. The value of the world's ecosystem services and natural capital. *Nature* **1997**, *387*, 253–260. [CrossRef]
4. Wang, Z.; Wu, J.; Madden, M.; Mao, D. China's wetlands: Conservation plans and policy impacts. *Ambio* **2012**, *41*, 782–786. [CrossRef] [PubMed]
5. Regnier, P.; Friedlingstein, P.; Ciais, P.; Mackenzie, F.T.; Gruber, N.; Janssens, I.A.; Laruelle, G.G.; Lauerwald, R.; Luyssaert, S.; Andersson, A.J. Anthropogenic perturbation of the carbon fluxes from land to ocean. *Nat. Geosci.* **2013**, *6*, 597–607. [CrossRef]
6. Duarte, C.M.; Losada, I.J.; Hendriks, I.E.; Mazarrasa, I.; Marbà, N. The role of coastal plant communities for climate change mitigation and adaptation. *Nat. Clim. Change* **2013**, *3*, 961–968. [CrossRef]
7. Rogers, K.; Kelleway, J.J.; Saintilan, N. The present, past and future of blue carbon. *Camb. Prism. Coast. Futur.* **2023**, *1*, e30. [CrossRef]
8. Macreadie, P.I.; Costa, M.D.; Atwood, T.B.; Friess, D.A.; Kelleway, J.J.; Kennedy, H.; Lovelock, C.E.; Serrano, O.; Duarte, C.M. Blue carbon as a natural climate solution. *Nat. Rev. Earth Environ.* **2021**, *2*, 826–839. [CrossRef]
9. Howard, J.; Sutton-Grier, A.; Herr, D.; Kleypas, J.; Landis, E.; Mcleod, E.; Pidgeon, E.; Simpson, S. Clarifying the role of coastal and marine systems in climate mitigation. *Front. Ecol. Environ.* **2017**, *15*, 42–50. [CrossRef]
10. Griggs, G.; Reguero, B.G. Coastal adaptation to climate change and sea-level rise. *Water* **2021**, *13*, 2151. [CrossRef]
11. Aitali, R.; Snoussi, M.; Kolker, A.S.; Oujidi, B.; Mhammdi, N. Effects of land use/land cover changes on carbon storage in North African Coastal Wetlands. *J. Mar. Sci. Eng.* **2022**, *10*, 364. [CrossRef]

12. Chi, Y.; Liu, D.; Xie, Z. Zonal simulations for soil organic carbon mapping in coastal wetlands. *Ecol. Indic.* **2021**, *132*, 108291. [CrossRef]
13. Ou, Y.; Bao, Z.; Ng, S.T.; Song, W.; Chen, K. Land-use carbon emissions and built environment characteristics: A city-level quantitative analysis in emerging economies. *Land Use Policy* **2024**, *137*, 107019. [CrossRef]
14. Pugh, T.; Arneth, A.; Olin, S.; Ahlström, A.; Bayer, A.; Goldewijk, K.K.; Lindeskog, M.; Schurgers, G. Simulated carbon emissions from land-use change are substantially enhanced by accounting for agricultural management. *Environ. Res. Lett.* **2015**, *10*, 124008. [CrossRef]
15. Chang, X.; Xing, Y.; Wang, J.; Yang, H.; Gong, W. Effects of land use and cover change (LUCC) on terrestrial carbon stocks in China between 2000 and 2018. *Resour. Conserv. Recycl.* **2022**, *182*, 106333. [CrossRef]
16. Berhongaray, G.; Alvarez, R.; De Paepe, J.; Caride, C.; Cantet, R. Land use effects on soil carbon in the Argentine Pampas. *Geoderma* **2013**, *192*, 97–110. [CrossRef]
17. Girmay, G.; Singh, B.; Mitiku, H.; Borresen, T.; Lal, R. Carbon stocks in Ethiopian soils in relation to land use and soil management. *Land Degrad. Dev.* **2008**, *19*, 351–367. [CrossRef]
18. He, C.; Zhang, D.; Huang, Q.; Zhao, Y. Assessing the potential impacts of urban expansion on regional carbon storage by linking the LUSD-urban and InVEST models. *Environ. Model. Softw.* **2016**, *75*, 44–58. [CrossRef]
19. Wiesmeier, M.; Prietzel, J.; Barthold, F.; Spörlein, P.; Geuß, U.; Hangen, E.; Reischl, A.; Schilling, B.; von Lützow, M.; Kögel-Knabner, I. Storage and drivers of organic carbon in forest soils of southeast Germany (Bavaria)–Implications for carbon sequestration. *For. Ecol. Manag.* **2013**, *295*, 162–172. [CrossRef]
20. Li, P.; Chen, J.; Li, Y.; Wu, W. Using the InVEST-PLUS model to predict and analyze the pattern of ecosystem carbon storage in Liaoning Province, China. *Remote Sens.* **2023**, *15*, 4050. [CrossRef]
21. Dangulla, M.; Abd Manaf, L.; Ramli, M.F.; Yacob, M.R.; Namadi, S. Exploring urban tree diversity and carbon stocks in Zaria Metropolis, North Western Nigeria. *Appl. Geogr.* **2021**, *127*, 102385. [CrossRef]
22. Zhang, C.; Song, T.; Shi, R.; Hou, Z.; Wu, N.; Zhang, H.; Zhuo, W. Estimating the Forest Carbon Storage of Chongming Eco-Island, China, Using Multisource Remotely Sensed Data. *Remote Sens.* **2023**, *15*, 1575. [CrossRef]
23. Kong, R.; Zhang, Z.; Zhang, F.; Tian, J.; Chang, J.; Jiang, S.; Zhu, B.; Chen, X. Increasing carbon storage in subtropical forests over the Yangtze River basin and its relations to the major ecological projects. *Sci. Total Environ.* **2020**, *709*, 136163. [CrossRef]
24. Guan, Q.; Chen, L.; Wang, Q.; Guan, C.; Li, H. Dynamical Identification of Urban-Rural Gradient and Ecosystem Service Response: A Case Study of Jinghong City, China. *Land* **2024**, *13*, 306. [CrossRef]
25. Zhao, M.; He, Z.; Du, J.; Chen, L.; Lin, P.; Fang, S. Assessing the effects of ecological engineering on carbon storage by linking the CA-Markov and InVEST models. *Ecol. Indic.* **2019**, *98*, 29–38. [CrossRef]
26. Wang, C.; Luo, J.; Qing, F.; Tang, Y.; Wang, Y. Analysis of the driving force of spatial and temporal differentiation of carbon storage in Taihang Mountains based on InVEST model. *Appl. Sci.* **2022**, *12*, 10662. [CrossRef]
27. Wang, Q.; Watanabe, M.; Ouyang, Z. Simulation of water and carbon fluxes using BIOME-BGC model over crops in China. *Agric. For. Meteorol.* **2005**, *131*, 209–224. [CrossRef]
28. Goetz, S.J.; Baccini, A.; Laporte, N.T.; Johns, T.; Walker, W.; Kellndorfer, J.; Houghton, R.A.; Sun, M. Mapping and monitoring carbon stocks with satellite observations: A comparison of methods. *Carbon Balance Manag.* **2009**, *4*, 2. [CrossRef] [PubMed]
29. Potter, C.; Klooster, S.; Genovese, V.; Hiatt, C. Forest production predicted from satellite image analysis for the Southeast Asia region. *Carbon Balance Manag.* **2013**, *8*, 9. [CrossRef] [PubMed]
30. Sun, J.; Mao, F.; Du, H.; Li, X.; Xu, C.; Zheng, Z.; Teng, X.; Ye, F.; Yang, N.; Huang, Z. Improving the Simulation Accuracy of the Net Ecosystem Productivity of Subtropical Forests in China: Sensitivity Analysis and Parameter Calibration Based on the BIOME-BGC Model. *Forests* **2024**, *15*, 552. [CrossRef]
31. Braakhekke, M.C.; Doelman, J.C.; Baas, P.; Müller, C.; Schaphoff, S.; Stehfest, E.; Van Vuuren, D.P. Modeling forest plantations for carbon uptake with the LPJmL dynamic global vegetation model. *Earth Syst. Dyn.* **2019**, *10*, 617–630. [CrossRef]
32. Zhang, Y.; Liao, X.; Sun, D. A Coupled InVEST-PLUS Model for the Spatiotemporal Evolution of Ecosystem Carbon Storage and Multi-Scenario Prediction Analysis. *Land* **2024**, *13*, 509. [CrossRef]
33. Li, H.; Guan, Q.; Fan, Y.; Guan, C. Ecosystem Service Value Assessment of the Yellow River Delta Based on Satellite Remote Sensing Data. *Land* **2024**, *13*, 276. [CrossRef]
34. Chen, Y.; Xu, Y.; Chen, T.; Zhang, F.; Zhu, S. Exploring the Spatiotemporal Dynamics and Driving Factors of Net Ecosystem Productivity in China from 1982 to 2020. *Remote Sens.* **2023**, *16*, 60. [CrossRef]
35. Zhang, L.; Xiong, L.; Li, J.; Huang, X. Long-term changes of nutrients and biocenoses indicating the anthropogenic influences on ecosystem in Jiaozhou Bay and Daya Bay, China. *Mar. Pollut. Bull.* **2021**, *168*, 112406. [CrossRef] [PubMed]
36. Tian, Y.; Li, J.; Wang, S.; Ai, B.; Cai, H.; Wen, Z. Spatio-temporal changes and driving force analysis of wetlands in Jiaozhou Bay. *J. Coast. Res.* **2022**, *38*, 328–344. [CrossRef]
37. Xu, N.; Gong, P. Significant coastline changes in China during 1991–2015 tracked by Landsat data. *Sci. Bull.* **2018**, *63*, 883–886. [CrossRef] [PubMed]
38. *Compilation Group of the Concise Rules for the Comprehensive Survey of Coastal Zone and Tideland Resources in China: Concise Rules for the Comprehensive Survey of Coastal Zone and Tideland Resources in China*; Ocean Press: Beijing, China, 1986.

39. Yang, J.; Huang, X. The 30 m Annual Land Cover Dataset and Its Dynamics in China from 1990 to 2019. *Earth Syst. Sci. Data* **2021**, *13*, 3907–3925. [CrossRef]
40. Breiman, L. Random forests. *Mach. Learn.* **2001**, *45*, 5–32. [CrossRef]
41. Caruana, R.; Niculescu-Mizil, A. An empirical comparison of supervised learning algorithms. In Proceedings of the 23rd International Conference on Machine Learning, Pittsburgh, PA, USA, 25–29 June 2006; pp. 161–168.
42. Guan, H.; Sun, Z.; Zhao, A. Spatio-temporal evolution and influencing factors of net carbon sink in marine aquaculture in China. *Front. Environ. Sci.* **2022**, *10*, 978073. [CrossRef]
43. Potter, C.S.; Randerson, J.T.; Field, C.B.; Matson, P.A.; Vitousek, P.M.; Mooney, H.A.; Klooster, S.A. Terrestrial ecosystem production: A process model based on global satellite and surface data. *Glob. Biogeochem. Cycles* **1993**, *7*, 811–841. [CrossRef]
44. Zhu, W.-Q.; Pan, Y.-Z.; Zhang, J.-S. Estimation of net primary productivity of Chinese terrestrial vegetation based on remote sensing. *Chin. J. Plant Ecol.* **2007**, *31*, 413.
45. Zheng, Z.; Zhu, W.; Zhang, Y. Seasonally and spatially varied controls of climatic factors on net primary productivity in alpine grasslands on the Tibetan Plateau. *Glob. Ecol. Conserv.* **2020**, *21*, e00814. [CrossRef]
46. Huo, H.; Sun, C. Spatiotemporal variation and influencing factors of vegetation dynamics based on Geodetector: A case study of the northwestern Yunnan Plateau, China. *Ecol. Indic.* **2021**, *130*, 108005. [CrossRef]
47. Wang, J.F.; Li, X.H.; Christakos, G.; Liao, Y.L.; Zhang, T.; Gu, X.; Zheng, X.Y. Geographical detectors-based health risk assessment and its application in the neural tube defects study of the Heshun Region, China. *Int. J. Geogr. Inf. Sci.* **2010**, *24*, 107–127. [CrossRef]
48. Wang, J.-F.; Hu, Y. Environmental health risk detection with GeogDetector. *Environ. Model. Softw.* **2012**, *33*, 114–115. [CrossRef]
49. Wang, J.; Xu, C.D. Geodetector: Principle and prospective. *Acta Geogr. Sin.* **2017**, *72*, 116–134.
50. Wang, J.-F.; Zhang, T.-L.; Fu, B.-J. A measure of spatial stratified heterogeneity. *Ecol. Indic.* **2016**, *67*, 250–256. [CrossRef]
51. Yu, Y.; Fang, S.; Zhuo, W. Revealing the Driving Mechanisms of Land Surface Temperature Spatial Heterogeneity and Its Sensitive Regions in China Based on GeoDetector. *Remote Sens.* **2023**, *15*, 2814. [CrossRef]
52. Schober, P.; Boer, C.; Schwarte, L.A. Correlation coefficients: Appropriate use and interpretation. *Anesth. Analg.* **2018**, *126*, 1763–1768. [CrossRef]
53. Zhang, Y.; Huang, D.; Jin, X.; Li, L.; Wang, C.; Wang, Y.; Pellissier, L.; Johnson, A.C.; Wu, F.; Zhang, X. Long-term wetland biomonitoring highlights the differential impact of land use on macroinvertebrate diversity in Dongting Lake in China. *Commun. Earth Environ.* **2024**, *5*, 32. [CrossRef]
54. Zamora, S.; Zitácuaro-Contreras, I.; Betanzo-Torres, E.A.; Herazo, L.C.S.; Sandoval-Herazo, M.; Vidal-Álvarez, M.; Marín-Muñiz, J.L. Carbon Pool in Mexican Wetland Soils: Importance of the Environmental Service. *Life* **2022**, *12*, 1032. [CrossRef] [PubMed]
55. Sjögersten, S.; De La Barreda-Bautista, B.; Brown, C.; Boyd, D.; Lopez-Rosas, H.; Hernández, E.; Monroy, R.; Rincón, M.; Vane, C.; Moss-Hayes, V. Coastal wetland ecosystems deliver large carbon stocks in tropical Mexico. *Geoderma* **2021**, *403*, 115173. [CrossRef]
56. Uniyal, S.; Purohit, S.; Chaurasia, K.; Rao, S.S.; Amminedu, E. Quantification of carbon sequestration by urban forest using Landsat 8 OLI and machine learning algorithms in Jodhpur, India. *Urban For. Urban Green.* **2022**, *67*, 127445. [CrossRef]
57. Ballut-Dajud, G.A.; Sandoval Herazo, L.C.; Fernández-Lambert, G.; Marín-Muñiz, J.L.; López Méndez, M.C.; Betanzo-Torres, E.A. Factors affecting wetland loss: A review. *Land* **2022**, *11*, 434. [CrossRef]
58. Muche, M.; Yemata, G.; Molla, E.; Adnew, W.; Muasya, A.M. Land use and land cover changes and their impact on ecosystem service values in the north-eastern highlands of Ethiopia. *PLoS ONE* **2023**, *18*, e0289962. [CrossRef] [PubMed]
59. Smith, P.; House, J.I.; Bustamante, M.; Sobocká, J.; Harper, R.; Pan, G.; West, P.C.; Clark, J.M.; Adhya, T.; Rumpel, C. Global change pressures on soils from land use and management. *Glob. Change Biol.* **2016**, *22*, 1008–1028. [CrossRef] [PubMed]
60. Yu, D.; Shi, P.; Shao, H.; Zhu, W.; Pan, Y. Modelling net primary productivity of terrestrial ecosystems in East Asia based on an improved CASA ecosystem model. *Int. J. Remote Sens.* **2009**, *30*, 4851–4866. [CrossRef]
61. Wang, Y.; Xu, X.; Huang, L.; Yang, G.; Fan, L.; Wei, P.; Chen, G. An improved CASA model for estimating winter wheat yield from remote sensing images. *Remote Sens.* **2019**, *11*, 1088. [CrossRef]
62. Wu, C.; Chen, K.; You, X.; He, D.; Hu, L.; Liu, B.; Wang, R.; Shi, Y.; Li, C.; Liu, F. Improved CASA model based on satellite remote sensing data: Simulating net primary productivity of Qinghai Lake basin alpine grassland. *Geosci. Model Dev.* **2022**, *15*, 6919–6933. [CrossRef]
63. Chuai, X.; Huang, X.; Lai, L.; Wang, W.; Peng, J.; Zhao, R. Land use structure optimization based on carbon storage in several regional terrestrial ecosystems across China. *Environ. Sci. Policy* **2013**, *25*, 50–61. [CrossRef]
64. Li, Y.; Qiu, J.; Li, Z.; Li, Y. Assessment of blue carbon storage loss in coastal wetlands under rapid reclamation. *Sustainability* **2018**, *10*, 2818. [CrossRef]
65. Ma, T.; Li, X.; Bai, J.; Ding, S.; Zhou, F.; Cui, B. Four decades' dynamics of coastal blue carbon storage driven by land use/land cover transformation under natural and anthropogenic processes in the Yellow River Delta, China. *Sci. Total Environ.* **2019**, *655*, 741–750. [CrossRef] [PubMed]
66. Yang, Y.; Li, H.; Qian, C. Analysis of the implementation effects of ecological restoration projects based on carbon storage and eco-environmental quality: A case study of the Yellow River Delta, China. *J. Environ. Manag.* **2023**, *340*, 117929. [CrossRef] [PubMed]
67. Zheng, H.; Zheng, H. Assessment and prediction of carbon storage based on land use/land cover dynamics in the coastal area of Shandong Province. *Ecol. Indic.* **2023**, *153*, 110474. [CrossRef]

68. Zhi, L.; Gou, M.; Li, X.; Bai, J.; Cui, B.; Zhang, Q.; Wang, G.; Bilal, H.; Abdullahi, U. Effects of sea level rise on land use and ecosystem services in the Liaohe delta. *Water* **2022**, *14*, 841. [CrossRef]
69. Zhu, L.; Song, R.; Sun, S.; Li, Y.; Hu, K. Land use/land cover change and its impact on ecosystem carbon storage in coastal areas of China from 1980 to 2050. *Ecol. Indic.* **2022**, *142*, 109178. [CrossRef]